Solution-proceed Air-stable Copper Bismuth Iodide CuBiI$_4$ for Photovoltaics

Zhaosheng Hu,*[a] Zhen Wang, [a] Gaurav Kapil, [a] Tingli Ma, [a] Satoshi Iikubo, [a] Takashi Minemoto,[b] Kenji Yoshino,[c] Taro Toyoda,[d] Qing Shen[d] and Shuzi Hayase*[a]

Abstract: Bismuth based solar cells have been under intensive interest as an efficient non-toxic absorber in photovoltaics. Within this new family of semiconductors, we herein, report a new, long-term stable material copper bismuth iodide (CuBiI$_4$). A solution-processed method is provided under air atmosphere. The adopted HI assisted Dimethylacetamide (DMA) co-solvent can completely dissolve CuI and BiI$_3$ powders with high concentration compared to other organic solvent. Moreover, high vapor pressure of Tributyl phosphate, we select for the solvent vapor annealing SVA, enable the whole low-temperature (≤70^{0}C) film preparation. It results in a stable, uniform dense CuBiI$_4$ film. The average grains size increasing with precursor concentration, greatly enlarge the PL life time and hall mobility. And carrier lifetime of 3.03 ns as well as an appreciable hall mobility of 110 cm^2/Vs were obtained. X-ray diffraction illustrates that the crystal structure is cubic (space group Fd3m) and favored in *[1, 1, 1]* direction. Moreover, the photovoltaic performance of CuBiI$_4$ was also investigated. A wide-bandgap (2.67 eV) solar cell with 0.82 % performance is presented, which shows an excellent long-term stability at least over 1008 hours under ambient conditions. This air-stable material may give an application in future tandem solar cells as a stable short-wavelength light absorber.

Introduction

The past decade has witnessed the boost improvement of solution-processed solar cells (SCs), especially the MAPbI$_3$ SCs, which are large-area, low-cost and high-performance.[1] However, the toxicity of lead limits their commercial potential. So, a lot of researches are forced on the candidates especially MASnI$_3$ SCs with about 8% power conversion efficiency (PCE).[2] But devices processing was usually conducted in a nitrogen-filled glovebox because of

the instability of tin cation, which is prone to disproportionation or oxidation after exposure to air and moisture.[3] Considering the instability as well as raising toxicity concerns, bismuth this non-toxic atom based materials are the most promising light-harvesting materials to replace lead and tin.[4] And, so far, incorporation of methylammonium (MA) and cesium in bismuth iodide complex are synthesized.[5] And silver bismuth iodide are reported.[6] Compared to the relative unstable organic cations such as MA, inorganic copper cation is stable. Moreover, copper is more abundant than the frequently used inorganic metal cations cesium and silver in earth, which is beneficial for applications. Monovalent copper cation has been mentioned before[16] and meanwhile, copper iodide is very stable and developed as a hole transport material. But recently there are no reports of photovoltaics of copper bismuth iodide. Herein, we firstly report a new solution-processed air-stable CuBiI$_4$ thin-film for photovoltaics.

Results and Discussion

Bismuth based devices, unlike lead or tin based solar cells, always suffer low coverage, poor morphology and pinholes in the resulting film.[7] Herein, we use HI acid assisted organic solvent to dissolve CuI and BiI$_3$ (see Experimental Section). HI acid reported to dissolve BiI$_3$ or CuI to synthesize or make bulk crystals,[8] is also used as the additive with small amount in organic solvent to improve the morphology in MAPbI$_3$ SCs[9]. As shown in **Figure S1,** concentrated HI acid (57 wt. %) assisted DMA completely dissolve CuI and BiI$_3$ powders with the exact molar ratio (HI: CuI: BiI$_3$=2: 1: 1) and form optically transparent, homogeneous solutions. It is mainly attributable to the high solubility of the produced complexes of hydrogen diiodocuprate(I) (HCuI$_2$) and hydrogen tetraiodobismuthanuide (HBiI$_4$) in DMA, which enable the up to 0.7 M concentration of CuI/BiI3. After one-step spin-coating, precursor solution yields a clear origin intermediates of DMA-HCuI$_2$-HBiI$_4$ covering the whole surface of substrate **(Figure 1i)**. Initial reports indicate that the much faster complete crystallization of Bi based films than Pb based films leads to the easily generated poor morphology.[10] Therefore, to suppress the fast evaporation rate of solvent and crystallization, solvent vapor annealing (SVA)[11] is applied. High vapor pressure of TBP, we select for SVA, enable the whole low-temperature film preparation. **Figure 1i-1ii** shows the obviously changed color of the film before and after SVA and following post-annealing at 70^{0}C for 30min. The FTIR spectrum of as-prepared film (that is, non-SVA) **(Figure 1)** illustrates the strong transmittance peaks for C=O stretching (1650 cm^{-1}), C-H stretching (2937 cm^{-1}), N-CH$_3$ (1397 cm^{-1}), C-CH$_3$ rocking (1014 cm^{-1}).[12] And it also includes the peaks associated with hydrogen bond of the added HI (1180 cm^{-1}-1360 cm^{-1})[13] and water (1634

[a] Dr. Z. Hu, Z. Wang, G. Kail, Prof. T. Ma, Assoc. Prof. S. Iikubo, Prof. S. Hayase
Graduate School of Life Science and Systems Engineering
Kyushu Institute of Technology
2-4 Hibikino, Waka-matsu-ku, Kitakyushu 808-0196, Japan
Email: hu-zhaosheng@edu.life.kyutech.ac.jp
        hayase@life.kyutech.ac.jp
[b] Prof. T. Minemoto
Department of Electrical and Electronic Engineering
Ritsumeikan University
1-1-1 Nojihigashi, Kusatsu, Shiga 525-8577, Japan
[c] Dr. K. Yoshino
Department of Electrical and Electronic Engineering
University of Miyazaki
Gakuenkibanadainishi, Miyazaki, Miyazaki Prefecture 899-2192, Japan
[d] Prof. T. Toyoda, Prof. Q. Shen
Department of Engineering Science
The University of Electro-Communications
1-5-1 Chofugaoka, Chofu, Tokyo 182-8585, Japan
Supporting information for this article is given via a link at the end of the document.

cm^{-1}[14]. The final film shows no transmittance peaks for organic molecular, which demonstrate the complete removal of the co-solvent.

form of a cation four-coordinated with the tetrahedral iodide groups and a bismuth cation is six-coordinated with the hexahedral iodide groups (**Figures 2c-2d**).
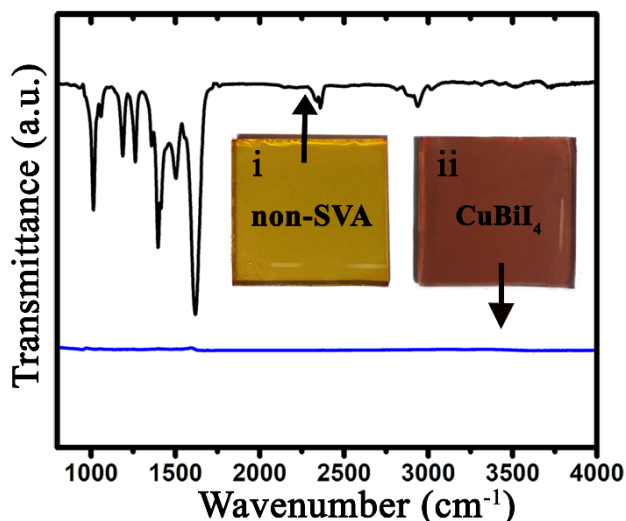

Figure 1 FTIR spectrum and photo images of the sample after one-step spin-coating precursor solution before SVA and sample dealt with SVA and the following post-annealing at 70 ^{0}C for 30min.

X-ray diffraction (XRD) spectra was measured to precisely determine the crystal structure of the grown crystal grains. Fitting the experimental data (**Figure 2a**) of Cu-Bi-I film prepared at 0.7 M precursor concentration and the XRD patterns (**Figure S3**) at other concentrations to the calculated XRD pattern from reference CIF file (ASM International & Material Phases Data System No.1123303), all the matched XRD peaks indicate CuBiI$_4$ films with cubic structure (space group Fd3m). The experimental cell parameters of a = 12.138 (2) Å , b = 12.127 (3) Å , c = 12.129 (2) Å are obtained. The little difference of parameters with the normal lattice parameters of a=b=c=12.134 Å are due to the internal horizontal strains of the thin-film because of the different thermal expansion coefficients. For the CuBiI$_4$ film at 0.7 M, there exist high-index crystal planes as well as the low-index planes in [*1, 1, 1*] crystal direction with 2θ peaks at 12.8^0, 25.5^0, 38.6^0, 52.1^0, which are (*1, 1, 1*), (*2, 2, 2*), (*3, 3, 3*) and (*4, 4, 4*) crystal planes respectively. It includes the relative weak peak of (*3, 1, 1*) crystal plane at 24.4^0. The low-index crystal phases possess very strong intensity and meanwhile, low full width at half maximum (FWHM) (0.10^0 for (*1, 1, 1*) and 0.15^0 for (*2, 2, 2*)). It demonstrates the grown crystals are high quality and favored in [*1, 1, 1*] direction. The CuBiI$_4$ film is highly air- and moisture-stable showing neither structure change nor phase separation after exposure in ambient conditions for 1008 hours (**Figure S2**). The structure of CuBiI$_4$ crystal cell is illustrated using the computer program VESTA (**Figure 2b**). The unit cell of CuBiI$_4$ with the cubic structure is densely and symmetrically composed of the copper, bismuth, and iodide. Both copper and bismuth metal ion in the unit cell displays a coordination polyhedron of iodides.[15] Copper is in the
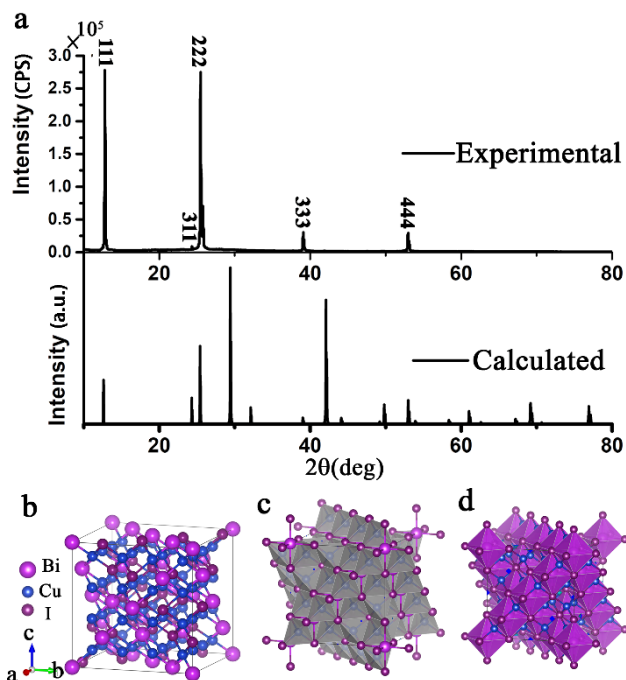
Figure 2 (a) Experimental XRD pattern and calculated XRD pattern from CIF No.1123303 of CuBiI$_4$. (b) Schematic of crystal cell of CuBiI$_4$ with cubic structure and the dimensions (a= 12.134 Å). (c)-(d) Copper and bismuth ions represented in polyhedral model respectively.

The crystallization of CuBiI$_4$ is very sensitive to precursor concentration. **Figure S3** shows a series of XRD patterns for solution-processed CuBiI$_4$ thin-films as a function of precursor concentration from 0.4 M-0.7 M. We confirm that [1, 1, 1] is the preferred crystallographic orientation for each concentration, while high concentration yields high quality, pin-hole free and dense grains with less other orientations. In addition, the surface morphologies were characterized by scanning electron microscopic (SEM). **Figure 3a** illustrates that up to 0.6 M especially 0.7 M produces a dense, uniform and pin-holes free copper bismuth iodide film. The average grain size greatly increase from 150 nm at 0.4 M to 300 nm at 0.7 M (**Table 1**), a finding that is consistent with the reported MAPbI$_3$ film dealt with SVA.[16] Moreover, compared to SVA method, **Figure S4** shows that the coper bismuth iodide film prepared by conventional thermal annealing at 0.7 M precursor concentration has lots of pin-holes and cannot form the obvious crystallized surface morphology, which agrees well with the observed XRD pattern (**Figure S3**). It demonstrates that SVA plays an important role in the crystallization.

The optical absorption (**Figure 4a**) of CuBiI4 obtained via UV/Vis spectroscopy increase with the precursor concentration. As shown in the Tauc plot (**Figure 4b**), we obtained an energy band gap Eg of 2.67 eV for CuBiI$_4$ assuming a direct band gap. In

Concentration (M)	0.4	0.5	0.6	0.7
Thickness (nm)	150	196	245	303
Average grain size (nm)	130	191	242	300
$<\tau>$ (ns)	0.23028	0.823027	1.66747	3.03371
Carrier concentration (cm^{-3})	2.47×10^{14}	5.75×10^{14}	6.03×10^{14}	6.56×10^{14}
Hall Mobility (cm^2/Vs)	33.3	48.2	88.4	110
Resistivity (Ωcm)	7.59×10^2	2.25×10^2	1.17×10^2	0.862×10^2

order to determine the energy band structure of $CuBiI_4$, photoelectron spectroscopy in air (PESA) was used to measure valence band energy (E_v) level (**Figure 4c**). The spectrum shows that E_v is at -5.68 eV. The conduction band energy level is found to be about -3.01 eV estimated by the equation $E_g = E_v - E_c$. Fermi level estimated by Kelvin probe is at -4.57 eV. Additionally, just like many other bismuth based active materials, such as silver bismuth iodide[6a] and double perovskite $Cs_2AgBiBr_6$,[4b] $CuBiI_4$ also presents weak indirect absorption from around 500 nm to 680 nm (Supporting Information, **Figure S5**) below the direct energy gap.
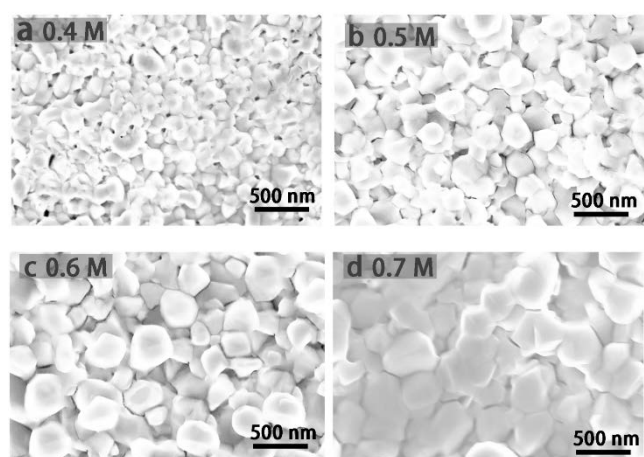

Figure 3 SEM images of solution-processed copper bismuth iodide thin-films as a function of precursor concentration.

Figure 4d illustrates that large grain size obtained at high precursor concentration enlarges the photoluminescence (PL) life time (steady PL is shown in **Figure S6**) from 0.23 ns to the highest 3.03 ns at 0.7 M (**Table 1**), which are obtained by the fitted stretch exponential decay function with curves. Such obvious increase is mainly because films with larger crystallites have smaller defect densities.[17] Moreover, both hall mobility and carrier concentration measured by Hall Effect shows the same tendency. An excellent hall mobility μ=110 cm^2/Vs and carrier concentration 6.56×10^{14} cm^{-3} at 0.7 M is obtained. It demonstrates that gain size of copper bismuth iodide plays an important role in the life time and hall mobility.

Table 1 Film thickness, grain size, average PL life time, carrier concentration, hall mobility, and resistivity of $CuBiI_4$ films on glass as a function of precursor concentration.
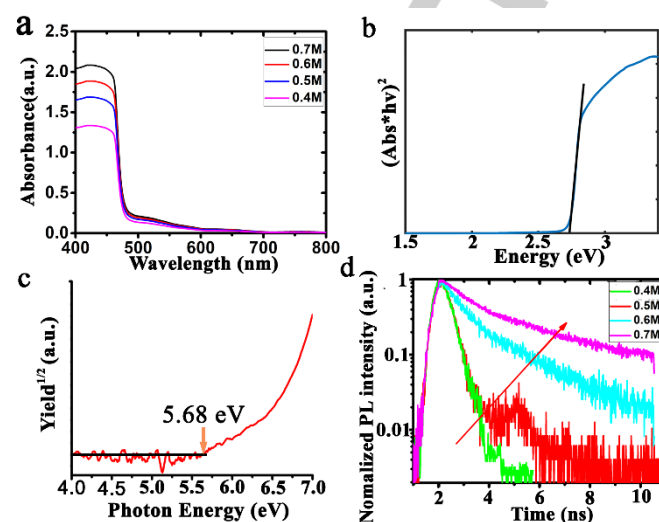

Figure 4 (a) UV/Vis spectra of copper bismuth iodide film. Inset: Tauc plot from absorbance spectra assuming direct energy band gap at 0.7 M. (b) Photon energy yield spectra in air. (c) Schematic of band structure of devices. (d) PL decay curves of $CuBiI_4$ depending on varied precursor solution concentration.

We also investigate the photovoltaic performance of the prepared $CuBiI_4$ devices of the structure FTO/compact TiO2/ mesoporous-TiO2 with CuBiI4/ Spiro-OMeTAD/ Gold. During the fabrication of devices, HI in such co-solvent almost have no influence on the substrate (**Figure S7**). **Figure 5a** shows the energy band diagram of devices. It illustrates that the TiO_2 and Spiro-OmeTAD are suitable for $CuBiI_4$ devices as hole transport layer and electron selective layer respectively. When exposed to light, the generated electron-hole pairs inside absorber layer can be separated and transported in devices. Precisely, electrons are selectively injected from $CuBiI_4$ (E_c: -3.01 eV) into TiO_2 (E_c: -4.0 eV) and then collected by FTO electrode (E_c: -4.4 eV), while holes are selectively transported from $CuBiI_4$ to Spiro-OMeTAD and finally collected by gold electrode.[1c, 18]

The performance of devices were measured in dark and under illumination using 100 $mWcm^2$, AM 1.5G covered with mask with light exposure area of 0.12 cm^2. **Figure 5b-5c** illustrates that high precursor concentration yields high power conversion efficiency (PCE), which is mainly attributable to the increase of short-circuit current density (Jsc). And, the change of fill factor (FF) and open-circuit voltage (Voc) is tiny. The highest PCE of 0.82% was obtained. As shown in **Figure S8,** films of $CuBiI_4$ with the mesoporous TiO_2 (diameter: 18nm) show the same tendency of average grain size. It demonstrates that high concentration and large grains are beneficial for photovoltaic performance. We also gave the photovoltaic performance of copper bismuth iodide prepared at 0.7 M precursor concentration by conventional thermal annealing (**Figure S9).** 0.03 % efficiency was obtained. Meanwhile, poor IPCE was observed. It demonstrates high

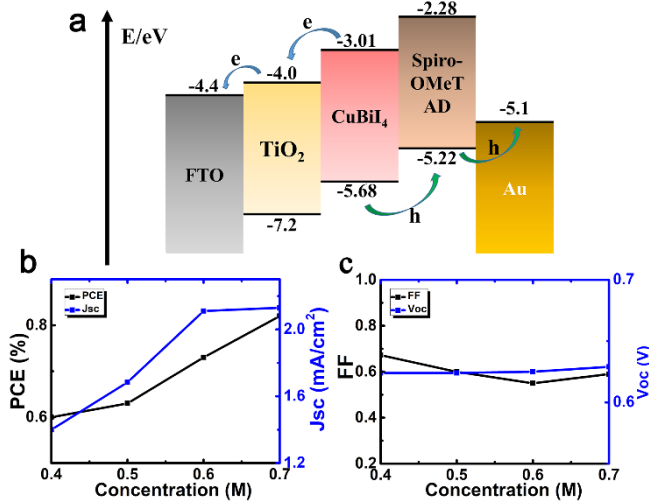quality film by SVA greatly improves the performance.

Figure 5 (a) Schematic energy band diagram of CuBiI₄ device. Energies are expressed in electron volts from vacuum level. Devices performance including (b) PCE, Jsc and (c) FF, Voc as a function of concentration of precursor solution.

Figure 6a shows J-V characteristics of device prepared with 0.7 M precursor concentration in two scan modes (forward and reverse) with illumination at 1 Sun. In forward scan mode (0V → Voc), the values of the Jsc, Voc and FF were found to be 2.19 mA/cm^2, 0.63 V and 0.57, respectively. In reverse scan mode (Voc → 0V), Jsc, Voc and FF were 2.17 mA/cm^2, 0.63 V and 0.59, respectively. The PCEs of the device in the forward as well as reverse scan mode are 0.82 % and 0.81 % respectively, which do not show obvious so-called hysteresis phenomena reported frequently in the perovskite solar cells[19]. The Incident Photon to Current Efficiency (IPCE) also emerge with about 465 nm wavelength, which closely support the direct energy gap of 2.67 eV (**Figure 6b**). And the integrated photocurrent density closely match with the IV curves. The copper bismuth iodide with relative wide (2.67 eV) energy bandgap processes comparable efficiency (0.82 %) with other bismuth based material, which as well as the >40 % appreciable IPCE within the range 300nm-465nm provides an effective wide-bandgap solar cell, which may provide an efficient short-wavelength absorber in future tandem solar cell. In this work, further increase of current density and open-circuit voltage represents the opportunity to obtain high performance. In addition, the used highest precursor concentration is limited by the water in the HI acid. Further improvement in the fabrication method can be expected to reduce the water amount in the solution by evaporate concentrated HI acid and incorporating pure HI molecular in DMA solvent.

Finally, the light-stability test were investigated under light intensity of 100 $mW \cdot cm^{-2}$ in ambient conditions with complete devices without encapsulation by JV sweep. Data is recorded every 168 hours. As shown in **Figure 6c** and **Figure 6d**, the PCE of devices maintain 89% over 1008 hours and show an

excellent stability. Meanwhile, CuBiI₄ film shows almost no degradation after such long-term storage in air, which demonstrate the mainly reason for the decrease of PCE may be the instability of Spiro-OMeTAD (**Figure S2**). Under encapsulation, more stable cell performance is expected.
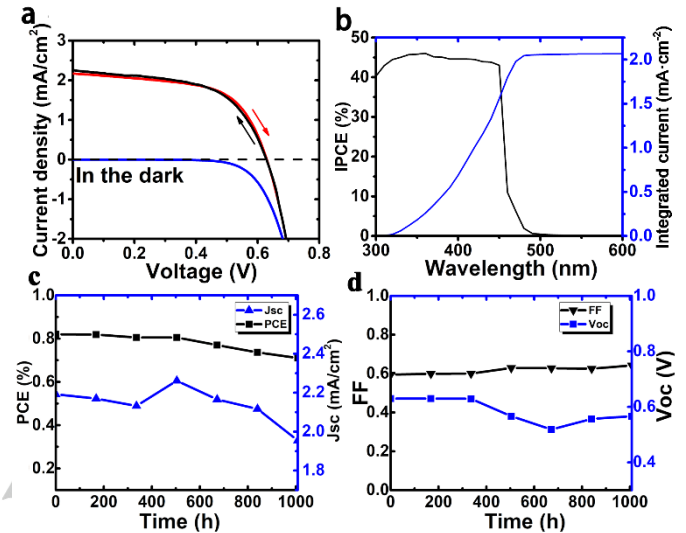

Figure 6 (a) J-V curve of CuBiI4 device (prepared at 0.7 M precursor solution), in which forward and reverse scan modes and dark are illustrated. (b) IPCE and integrated photocurrent of the devices. (c)-(d) Photovoltaic performance change during storage of devices under light intensity of 100 mW cm^{-2}.

Conclusions

In conclusion, solution-processed copper bismuth iodide films are easily fabricated using a one-step spin-coating followed by SVA and post-annealing under low temperature. The HI acid assisted DMA solvent highly dissolve CuI and BiI₃ powders and form clear solution with high concentration. CuBiI₄ films show a very long-term stability under air atmosphere. X-ray diffraction spectrum illustrates the high-index facets as well as low-index facets in *[1, 1, 1]* direction for high precursor concentration, which demonstrate the obtained high quality crystal grains. In addition, the cubic crystal cell with lattice constant observed shows that both copper and bismuth ions are in the form with four-coordinated and six-coordinated of iodide respectively. The concentration of precursor solution increases the average grain size of CuBiI₄ films, which meanwhile, greatly enlarges PL life time from 0.23ns to 3.03 ns at 0.7 M and increase the hall mobility to appreciable 110 cm^2/Vs.

Moreover, the photovoltaic performance of CuBiI₄ were investigated. A wide-bandgap (2.67 eV) solar cell with 0.82 % performance is presented, which shows an excellent long-term stability at least over 1008 hours under ambient conditions. This wide-bandgap material may provide an application in future tandem solar cells as a long-term stable short-wavelength light harvester.

Experimental Section

Materials preparation

N,N-dimethylacetamide (DMA) with the added Hydroiodic acid (HI) was employed to completely dissolve the BiI_3 and CuI powder. It must be noted that the added HI acid in organic solvent do not influence the FTO substrate. The detail preparation method is as follows. First, the high pure powder of CuI and BiI_3 are mixed with exactly molar ration 1:1 and added in 1ml DMA by stirring for 2h at room temperature with the concentration varied from 0.4 M to 0.7 M. After that, HI acid (57 wt. % without stabilizer) is added dropwise with stirring (4 h) to avoid the fast evaporation of HI molecular. The amount of the added HI in molar is two times of that of BiI_3 and the solution became clear and purple-black.

Devices fabrication

Figure 7 illustrated the fabrication of $CuBiI_4$ devices in details. F-doped tin oxide (FTO) substrates were cleaned in an ultrasonic bath by acetone, isopropyl alcohol and deionized water in turn for 30min respectively. Then, they are dried with nitrogen gas and sequentially cleaned by plasma. Compact-TiO_2 (**Figure 7i**) with about 50 nm thickness was sprayed on the substrates under 300 ^0C. After that, a mesoporous TiO_2 layer with thickness of about 250 nm (particle diameter: 18 nm) was spin-coated and annealed at 500 ^0C for 1.5 h. Then, the absorber layer was deposed by one-step method (**Figure 7ii**), in which about 80ul solution is casted on the surface and spin-coated with 500 rpm for 5 s and 5 krpm for 30 s. Solvent vapour annealing method was carried out with TBP solvent (**Figure 7iii**) at room temperature. As-prepared samples were put on the holder in a chamber and exposed to vapour of TBP. The distance between sample and the solvent and the amount of TDP are precisely tuned to crystallize $CuBiI_4$ crystals. The random holes inside the cap of the chamber for SVA can avoid the too much accumulation TBP on the surface of samples. After being annealed in TBP for about 2-3 h, samples were taken out from the chamber and dried on a hot plate under 70^0C for 30min to completely remove the remaining solvent (**Figure 7iv**). Then, HTM layer was fabricated by spin-coating Spiro-MeOTAD solution (**Figure 7v**). The solution was prepared by dissolving 72.3 mg of 2,2',7,7'-tetrakis-(N,N-di-p-methoxyphenyl-amine)-9,9'-spirobifluorene (spiro-MeOTAD, Merck), in 1ml of chlorobenzene, in which 80μl ethanol and 17.5 μl lithium bis(trifluoromethanesulfonyl)imide (Li-TFSI) solution (520 mg Li-TSFI in 1 ml acetonitrile (Sigma-Aldrich, 99.8%)) were added. It must be noted that, in this preparation, 4-tert-butyl pyridine (TBP) is not used because it dissolved the thin $CuBiI_4$ layer. And the added ethanol actually play the same role as TBP to dissolve Li-TSFI in chlorobenzene. Finally, about 100 nm gold electrode was deposited by thermal evaporator to complete the devices (**Figure 7vi**).
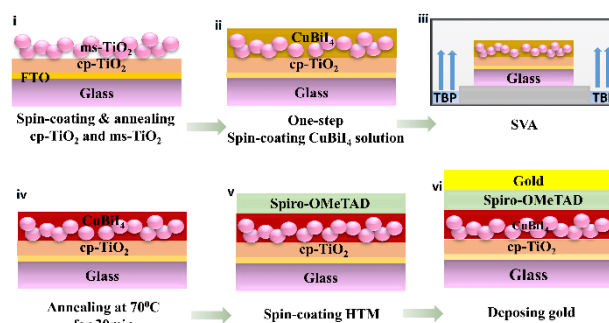

Figure 7 Schematic of fabrication process of $CuBiI_4$ solar cells.

$CuBiI_4$ thin-film fabrication

$CuBiI_4$ films were fabricated on glass substrate and the one-step spin-coating, SVA process and post annealing are same with the device fabrication.

Acknowledgements

**Keywords:** Copper bismuth iodide, $CuBiI_4$,   Solar cell.

[1]   aJ. Burschka, N. Pellet, S.-J. Moon, R. Humphry-Baker, P. Gao, M. K. Nazeeruddin, M. Grätzel, *Nature* **2013**, *499*, 316-319; bU. Bach, D. Lupo, P. Comte, J. Moser, F. Weissörtel, J. Salbeck, H. Spreitzer, M. Grätzel, *Nature* **1998**, *395*, 583-585; cZ. Hu, G. Kapil, H. Shimazaki, S. S. Pandey, T. Ma, S. Hayase, *The Journal of Physical Chemistry C* **2017**, *121*, 4214-4219; dN. J. Jeon, H. G. Lee, Y. C. Kim, J. Seo, J. H. Noh, J. Lee, S. I. Seok, *Journal of the American Chemical Society* **2014**, *136*, 7837-7840; eA. Dualeh, P. Gao, S. I. Seok, M. K. Nazeeruddin, M. Grätzel, *Chemistry of Materials* **2014**, *26*, 6160-6164.

[2]   aC. C. Stoumpos, C. D. Malliakas, M. G. Kanatzidis, *Inorganic chemistry* **2013**, *52*, 9019-9038; bT. K. Todorov, K. B. Reuter, D. B. Mitzi, *Advanced materials* **2010**, *22*; cM. H. Kumar, S. Dharani, W. L. Leong, P. P. Boix, R. R. Prabhakar, T. Baikie, C. Shi, H. Ding, R. Ramesh, M. Asta, *Advanced Materials* **2014**, *26*, 7122-7127; dD. Sabba, H. K. Mulmudi, R. R. Prabhakar, T. Krishnamoorthy, T. Baikie, P. P. Boix, S. Mhaisalkar, N. Mathews, *The Journal of Physical Chemistry C* **2015**, *119*, 1763-1767.

[3]   A. Babayigit, D. D. Thanh, A. Ethirajan, J. Manca, M. Muller, H.-G. Boyen, B. Conings, *Scientific reports* **2016**, *6*, 18721.

[4]   aA. J. Lehner, H. Wang, D. H. Fabini, C. D. Liman, C.-A. Hébert, E. E. Perry, M. Wang, G. C. Bazan, M. L. Chabinyc, R. Seshadri, *Applied Physics Letters* **2015**, *107*, 131109; bA. H. Slavney, T. Hu, A. M. Lindenberg, H. I. Karunadasa, *Journal of the American Chemical Society* **2016**, *138*, 2138-2141.

[5]   aR. L. Hoye, R. E. Brandt, A. Osherov, V. Stevanović, S. D. Stranks, M. W. Wilson, H. Kim, A. J. Akey, J. D. Perkins, R. C. Kurchin, *Chemistry-A European Journal* **2016**, *22*, 2605-2610; bB. W. Park, B. Philippe, X. Zhang, H. Rensmo, G. Boschloo, E. M. Johansson, *Advanced Materials* **2015**, *27*, 6806-6813; cZ. Xiao, W. Meng, D. B. Mitzi, Y. Yan, *The Journal of Physical Chemistry Letters* **2016**, *7*, 3903-3907; dM. Leng, Z. Chen, Y. Yang, Z. Li, K. Zeng, K. Li, G. Niu, Y. He, Q. Zhou, J. Tang, *Angewandte Chemie International Edition* **2016**, *55*, 15012-15016.

[6]   aY. Kim, Z. Yang, A. Jain, O. Voznyy, G. H. Kim, M. Liu, L. N. Quan, F. P. García de Arquer, R. Comin, J. Z. Fan, *Angewandte Chemie International Edition* **2016**, *55*, 9586-9590; bH. Zhu, M. Pan, M. B. Johansson, E. M. J. Johansson, *ChemSusChem* **2017**, *10*, 2592-2596.

[7]   A. J. Lehner, D. H. Fabini, H. A. Evans, C.-A. Hébert, S. R. Smock, J. Hu, H. Wang, J. W. Zwanziger, M. L. Chabinyc, R. Seshadri, *Chem. Mater* **2015**, *27*, 7137-7148.

[8]   M. Gu, P. Gao, X. L. Liu, S. M. Huang, B. Liu, C. Ni, R. K. Xu, J. M. Ning, *Crystal Research and Technology* **2010**, *45*, 365-370.

[9]   J. H. Heo, D. H. Song, H. J. Han, S. Y. Kim, J. H. Kim, D. Kim, H. W. Shin, T. K. Ahn, C. Wolf, T. W. Lee, *Advanced Materials* **2015**, *27*, 3424-3430.

[10]   aS. S. Shin, J. P. Correa Baena, R. C. Kurchin, A. Polizzotti, J. J. Yoo, S. Wieghold, M. G. Bawendi, T. Buonassisi, *Chemistry of Materials* **2018**, *30*, 336-343; bT. Singh, A. Kulkarni, M. Ikegami, T. Miyasaka, *ACS Applied Materials & Interfaces* **2016**, *8*, 14542-14547.

[11]   aB. Gholamkhass, P. Servati, *Organic Electronics* **2013**, *14*, 2278-2283; bC. D. Wessendorf, G. L. Schulz, A. Mishra, P. Kar, I. Ata, M. Weidelener, J. Urdanpilleta, J. Hanisch, E. Mena‐Osteritz, M. Lindén, *Advanced Energy Materials* **2014**, *4*.

[12]   aD. M. Verbovy, T. G. Smagala, M. A. Brynda, W. R. Fawcett, *Journal of Molecular Liquids* **2006**, *129*, 13-17; bG. Konstantatos, I. Howard, A. Fischer, S. Hoogland, J. Clifford, E. Klem, L. Levina, E. H. Sargent, *Nature* **2006**, *442*, 180-183.

[13]   C. Zhu, M. Tsuge, M. Räsänen, L. Khriachtchev, *The Journal of chemical physics* **2015**, *142*, 144306.

[14]   B. L. Mojet, S. D. Ebbesen, L. Lefferts, *Chemical Society Reviews* **2010**, *39*, 4643-4655.

[15]   P. Fourcroy, D. Carre, F. Thevet, J. Rivet, *Acta Crystallographica Section C: Crystal Structure Communications* **1991**, *47*, 2023-2025.

[16]   Z. Xiao, Q. Dong, C. Bi, Y. Shao, Y. Yuan, J. Huang, *Advanced Materials* **2014**, *26*, 6503-6509.

[17]   V. D'Innocenzo, A. R. Srimath Kandada, M. De Bastiani, M. Gandini, A. Petrozza, *Journal of the American Chemical Society* **2014**, *136*, 17730-17733.

[18]   M. Ye, C. He, J. Iocozzia, X. Liu, X. Cui, X. Meng, M. Rager, X. Hong, X. Liu, Z. Lin, *Journal of Physics D: Applied Physics* **2017**, *50*, 373002.

[19]   aS. Meloni, T. Moehl, W. Tress, M. Franckevičius, M. Saliba, Y. H. Lee, P. Gao, M. K. Nazeeruddin, S. M. Zakeeruddin, U. Rothlisberger, *Nature communications* **2016**, *7*, 10334; bE. Unger, E. Hoke, C. Bailie, W. Nguyen, A. Bowring, T. Heumüller, M. Christoforo, M. McGehee, *Energy & Environmental Science* **2014**, *7*, 3690-3698.

Entry for the Table of Contents

FULL PAPER

A solution-proceed air-stable CuBiI$_4$ and its long-term stable effective wide-bandgap solar cells are provided for future non-toxic photovoltaics.
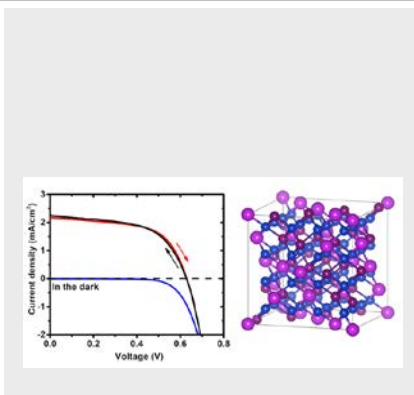
Zhaosheng Hu,* Zhen Wang, Gaurav Kapil, Tingli Ma, Satoshi Iikubo,Takashi Minemoto, Kenji Yoshino, Taro Toyoda, Qing Shen and Shuzi Hayase*